

### **RESEARCH PAPER**

# Deletion of maize RDM4 suggests a role in endosperm maturation as well as vegetative and stress-responsive growth

Shangang Jia<sup>1,2,3,o</sup>, Abou Yobi<sup>4</sup>, Michael J. Naldrett<sup>5,o</sup>, Sophie Alvarez<sup>5,o</sup>, Ruthie Angelovici<sup>4,o</sup>, Chi Zhang<sup>6</sup> and David R. Holding<sup>3,\*,o</sup>

- <sup>1</sup> College of Grassland Science and Technology, China Agricultural University, Beijing 100193, China
- <sup>2</sup> Key Laboratory of Pratacultural Science, Beijing Municipality, Yuanmingyuan West Road, Haidian District, Beijing 100193, China
- <sup>3</sup> Department of Agronomy and Horticulture, Center for Plant Science Innovation, Beadle Center for Biotechnology, University of Nebraska, Lincoln, NE 68588, USA
- <sup>4</sup> Bond Life Sciences Center, Division of Biological Sciences, Interdisciplinary Plant Group, University of Missouri, Columbia, MO 65201, USA
- <sup>5</sup> Proteomics and Metabolomics Core facility, University of Nebraska-Lincoln, Lincoln, NE 68588, USA
- <sup>6</sup> School of Biological Sciences, Center for Plant Science Innovation, Beadle Center for Biotechnology, University of Nebraska, Lincoln, NE 68588, USA

Received 7 April 2020; Editorial decision 1 July 2020; Accepted 10 July 2020

Editor: Andrea Braeutigam, Bielefeld University, Germany

#### **Abstract**

Opaque kernels in maize may result from mutations in many genes, such as *OPAQUE-2*. In this study, a maize null mutant of *RNA-DIRECTED DNA METHYLATION 4* (*RDM4*) showed an opaque kernel phenotype, as well as plant developmental delay, male sterility, and altered response to cold stress. We found that in opaque kernels, all zein proteins were reduced and amino acid content was changed, including increased lysine. Transcriptomic and proteomic analysis confirmed the zein reduction and proteomic rebalancing of non-zein proteins, which was quantitatively and qualitatively different from *opaque-2*. Global transcriptional changes were found in endosperm and leaf, including many transcription factors and tissue-specific expressed genes. Furthermore, of the more than 8000 significantly differentially expressed genes in wild type in response to cold, a significant proportion (25.9% in moderate cold stress and 40.8% in near freezing stress) were not differentially expressed in response to cold in *rdm4*, suggesting RDM4 may participate in regulation of abiotic stress tolerance. This initial characterization of maize *RDM4* provides a basis for further investigating its function in endosperm and leaf, and as a regulator of normal and stress-responsive development.

**Keywords:** Cold stress, endosperm, leaf, maize, Opaque mutant, RDM4, zein proteins.

# Introduction

Zein proteins make up the majority of maize (*Zea mays*) endosperm proteins, and the most abundant of those are the  $\alpha$ -zeins, which are encoded by highly duplicated gene families

(Holding and Messing, 2013). Through coordinated gene expression and specific interactions during the middle phase of endosperm development (Woo et al., 2001; Kim et al., 2002;

<sup>\*</sup> Correspondence: dholding2@unl.edu

Wu and Messing, 2010; Guo et al., 2013), zeins are organized into ER-localized and discretely organized proteins bodies (Lending and Larkins, 1989). Mutations that reduce zein abundance, either direct mutations or mutations of regulatory factors, result in changes to protein body shape, size, and number and partly or completely disrupt the formation of vitreous endosperm resulting in opaque kernels (Holding, 2014). Such opaque mutants include floury-1 (fl1) and opaque-1 (o1) (Holding et al., 2007; Wang et al., 2012). The most well-known of the maize opaque mutants is opaque-2 (o2), which has been widely studied because of its increased lysine and tryptophan content (Mertz et al., 1964). The amino acid improvements in o2 result from substantially reduced accumulation of lysine-devoid zeins and the compensatory increase in lysinecontaining non-zein proteins. Although the non-zein changes largely affect the proteome globally, discrete qualitative changes in especially lysine-rich proteins are also important (Morton et al., 2016). Cloning of the O2 gene revealed that it encodes a bZIP transcription factor that regulates α-zeins (Schmidt et al., 1990). O2 is now known to regulate most classes of zein genes (Li et al., 2015) and to act in concert with other transcription factors, OHP and PBF (Zhang et al., 2015). Furthermore, O2 plays a wider role in orchestrating storage acquisition in endosperm since it both directly and indirectly regulates several starch synthesis genes (Zhang et al., 2016).

The Arabidopsis RNA-DIRECTED DNAMETHYLATION 4 (RDM4) mutant shows a dwarf plant phenotype and vulnerability to cold stress (He et al., 2009; Chan et al., 2016). It also exhibits pleiotropic developmental abnormalities under normal growth conditions and extensive modification of the RNA polymerase II (Pol II)-mediated transcriptome, and the RDM4 protein was shown to associate with Pol II, Pol IV, and Pol V (Matzke et al., 2015). The complexity of the factors that interact with Pol II may provide differential transcription in response to specific biotic, abiotic and developmental scenarios. For example, the Arabidopsis rdm4 mutant showed diminished expression of several cold responsive genes under normal development, providing a clue that the gene is involved in adaptation to at least one abiotic stress (He et al., 2009). Subsequently, it was shown that cold hypersensitivity is one aspect of the pleiotropic rdm4 mutant phenotype and, most significantly, that the RDM4 protein directs Pol II transcription of these cold-responsive genes in an RNA-directed DNA methylation (RdDM)-independent manner (Chan et al., 2016). This raises the question of the possible involvement of RDM4 in cold responsiveness in other plant species including monocots. It also invites the question of whether RDM4 and other factors are involved in other transcriptional scenarios involving stress-related or tissue-specific gene expression such as in maize endosperm.

We previously used  $\gamma$ -radiation to create deletion mutants in the B73 background including opaque kernel mutants, and implemented a bulked segregant RNA-seq (BSR-seq) and exome-seq based mapping pipeline (Jia et al., 2016). We subsequently developed bulked segregant exome sequencing (BSEx-seq) for mapping and identifying a short deletion on chromosome 10 in mutant 1486 (Jia et al., 2018a, b). The causal deletion had an estimated size of 6248 bp with genomic

coordinates of two break points at 1 540 105 and 1 546 352, and covered three predicted genes (GRMZM2G098603, GRMZM2G098596, and GRMZM2G176546) based on the B73 genome assembly v3. The deletion was confirmed by our exome-seq analysis and genomic PCR (Jia et al., 2018b). In the present study, we established the causality of the loss of RDM4 for opaque kernel and plant phenotype in this mutant, henceforth named Zm-rdm4. Through characterization of its phenotype and changes of transcriptome and proteome, we highlight the differences between rdm4 and o2 in the nature of zein reduction and non-zein proteome rebalancing in the opaque kernel endosperm. We present leaf transcriptome data that may suggest an overarching regulatory role for RDM4 in contributing to tissue-specific and stress-related gene expression networks.

# Materials and methods

Sample collection for RNA-seq

The rdm4 mutant was created as previously described (Jia et al., 2016, 2018b), and grown in the greenhouse and field for collection of leaf and developing ears. For endosperm RNA-seq, 20 d after pollination (DAP) embryo DNA was extracted for genotyping according to a previously published method (Jia et al., 2018b) while endosperms were flash frozen in liquid nitrogen and stored at -80 °C. Wild type (WT), heterozygous and opaque mutant kernels were identified based on two genomic PCRs by using two primer pairs, RDM4\_E3F and RDM4\_E2R, for a 526-bp fragment inside the gene RDM4, and RDM4\_E5F and AMP\_E3R for fragments of only ~1 kb in rdm4 and ~7 kb in WT (see Supplementary Table S1 at JXB online). Endosperm RNAs genotyped for both homozygous WT and mutant types were extracted, processed by RNase-free DNase I, and purified using the Plant RNeasy Kit (Qiagen) for RNA-seq.

Seedling cold stress treatments were performed by first germinating the seeds in standard potting compost in 3-inch peat pots, growing in the greenhouse and subsequently in a Conviron growth chamber. The seedling28 treatment consisted of 14 d growth at 28 °C in the greenhouse (16 h day, 8 h night). For mild cold stress of seedling10, plants were grown at 28 °C for 11 d followed by 10 °C for 3 d. For severe cold stress of seedling2, seedlings were grown at 28 °C for 11 d, 10 °C for 3 d followed by 2 °C for 1 d. Wild type and mutant seedlings were determined based on both the seed opaque phenotype and leaf genomic DNA genotyping. DNA was extracted from leaves of ~14-day-old plants and genotyped for WT, heterozygous and mutant plants, before seedling RNA was extracted and purified for RNA-seq.

cDNA was synthesized for constructing Illumina sequencing libraries by using NEBNext® Ultra<sup>TM</sup> II DNA Library Prep (NEB, Ipswich, MA, USA). Groups of six endosperm and 18 seedling samples were sequenced for RNA-seq on separate HiSeq 2500 lanes, with a 125-bp paired-end run and v4 chemistry. The exome capture and sequencing were performed on pooled genomic DNA of 14-day-old normal and mutant seedlings by using SeqCap EZ Developer Maize Exome kit (Roche NimbleGen, Madison, WI, USA) (Jia et al., 2018b). All the sequencing was performed in the University of Minnesota Genomics Center. The data are deposited in the Short Reads Archive (SRA) database (http://www.ncbi.nlm.nih. gov/sra) of NCBI with the accession number of PRJNA306879.

#### Quantitative RT-PCR

We designed primers using Primer3 and our locally developed perl script for batch processing to do the RT-PCR and qRT-PCR (see Supplementary Table S1). Total RNA from endosperm and seedling was extracted by using the Plant RNeasy Kit (Qiagen) and DNase I treatment. First-strand complementary DNA was synthesized using the Bio-Rad iScript<sup>TM</sup> cDNA Synthesis Kit (Bio-Rad, Hercules, CA, USA). The qRT-PCR analyses were performed in a My iQ icycler (Bio-Rad) using

IQ SYBR Green super mix (Bio-Rad), with three biological replicates using maize gene Zm00001d018145 as an internal control since it was found to have invariant  $C_{\rm t}$  values between all samples. The relative transcript levels were determined using  $2^{-\Delta\Delta C_{\rm t}}$  method.

#### SDS-PAGE and LC-MS/MS analysis

Total protein as well as alcohol-soluble zein and aqueous non-zein fractions were extracted from mature endosperm according to a previous method (Wallace et al., 1990). Maize endosperm was ground, and then suspended in extraction buffer (12.5 mM Na-borate pH 10, 0.1% SDS, 1%  $\beta$ -mercaptoethanol). After pelleting insoluble material (such as starch), the supernatant was diluted in ethanol to 70% ethanol to precipitate the non-zein proteins. The non-zein protein pellet was washed three times with 70% ethanol, air dried, and stored at -80 °C. SDS-PAGE was used to compare single kernels of normal (i.e.WT and heterozygous) and mutant types. All the comparisons between the mature normal and mutant kernels were based on the same amount of kernel flour (Jia et al., 2016; Morton et al., 2016).

For LC-MS/MS analysis, kernels of 20 DAP were genotyped for homozygous mutant and WT alleles, with four replicates. Non-zein pellets were thawed and redissolved in 7 M urea, 2 M thiourea, and 5 mM DTT, and 100 µg of each sample was reduced at 37 °C for 2 h. Proteins were alkylated with 15 mM iodoacetamide, and then quenched with an equimolar amount of DTT. Samples were diluted 9-fold and subjected to trypsin digestion, before being redissolved in 0.1 M triethylammonium bicarbonate. Eighty micrograms of each sample was labeled with 0.8 mg of TMT10-plex reagent using labels 127N-130C only (Thermo Fisher Scientific, Waltham, MA, USA), combining all eight samples into one single 8-plex sample. Three hundred micrograms of this combined sample was sub-fractionated offline into 96 fractions using high pH reverse phase C18 chromatography (ACQUITY UPLC® CSH™ C18, 1.7 µm, 2.1×150mm, Waters Corp.) at pH 10 and then recombined to give a total of 12 fractions according to the previous strategy (Yang et al., 2012). Each of the 12 fractions from the high pH reverse phase run was analysed by LC-MS/MS on an RSLCnano system (Thermo Fisher Scientific) coupled to a Q-Exactive HF mass spectrometer (Thermo Fisher Scientific). The samples were first injected onto a trap column (Acclaim PepMap<sup>TM</sup> 100, 75 μm×2 cm, Thermo Fisher Scientific) for 3.3 min at a flow rate of 5 µl min<sup>-1</sup>, 2% acetonitrile, 0.1% formic acid before switching inline with the main column. Separation was performed on a C18 nano column (Acquity UPLC® M-class, Peptide CSHTM 130A, 1.7  $\mu$ m, 75  $\mu$ m×250 mm, Waters Corp.) at 260 nl min<sup>-1</sup> with a linear gradient from 5% to 35% over 96 min. The LC aqueous mobile phase contained 0.1% (v/v) formic acid in water and the organic mobile phase contained 0.1% (v/v) formic acid in 80% (v/v) acetonitrile. Mass spectra for the eluted peptides were acquired on a Q Exactive HF mass spectrometer in data-dependent mode using a mass range of m/z 375-1500, resolution 120 000, automatic gain control (AGC) target 3×10<sup>6</sup>, maximum injection time 60 ms for the MS1 peptide measurements. Data-dependent MS2 spectra were acquired by higher-energy collisional dissociation as a top15 experiment with a normalized collision energy set at 33%, AGC target set to 1×10<sup>5</sup>, 60 000 resolution, intensity threshold  $5\times10^4$  and a maximum injection time of 100 ms. Dynamic exclusion was set at 30 s and the isolation window set to 1.2 m/z to reduce co-isolation.

Data were analysed in Proteome Discoverer 2.2 software (Thermo Fisher Scientific) connected to Mascot 2.6.1, which searched the common contaminants database cRAP (116 entries, www.theGPM.org) and the Uniprot reference proteome database for *Z. mays* (ID: UP000007305 retrieved on 20171001, 99 369 entries). Peptides were validated by Percolator with a 0.01 posterior error probability (PEP) threshold. The data were searched using a decoy database to set the false discovery rate to 1%. The reporter abundance was normalized using total peptide amount. The protein ratios were calculated using summed abundance for each replicate separately and the geometric median of the resulting ratios was used as the protein ratios. The mass spectrometry proteomic data were deposited into the ProteomeXchange database via ProteomeXchange submission tool with the dataset identifier PXD016445.

Amino acid content analysis

Protein-bound and free amino acids were extracted and quantified according to a previously published method (Li *et al.*, 2018*a*; Yobi and Angelovici, 2018). The *in silico* calculation of amino acid content was conducted according to a previous publication (Morton *et al.*, 2016).

#### Data analysis

Structural variations were called by Lumpy (Layer et al., 2014) to help determine the deletion positions. RNA-seq data were analysed with the standard protocol with trimming, mapping by TopHat2 (Kim et al., 2013) on the maize genome assembly v4 (downloaded from ftp://ftp. ensemblgenomes.org/pub/plants/release-44/fasta/zea\_mays/dna/), and determining mRNA expression fragments per kilobase per million mapped reads (fpkm) values by Cufflinks (Trapnell et al., 2012). For functional enrichment analysis, a bin-wise Wilcoxon test in MapMan v3.6 was conducted (Usadel et al., 2006, 2009). R functions prcomp() and ggbiplot() were employed for principal component analysis (PCA) and visualization. Significantly differentially expressed genes (DEGs) and differential proteins (DPs) were identified by the R package DESeq2 (Love et al., 2014).

### Results

Opaque kernel and vegetative phenotypes result from deletion of RDM4

The maize deletion mutant rdm4 had apparently normal-sized opaque kernels for the mutant alleles (-/-), through which light cannot penetrate (Fig. 1A). The mutant was crossed with Mo17 to make an F<sub>2</sub> mapping population and confirm the robust heritability of the mutant opaque kernel phenotype since segregation of opaque and vitreous kernels occurred in F<sub>2</sub> ears (Fig. 1B). Self-pollinating the heterozygous F<sub>1</sub> plants containing rdm4 allele gave F2 kernels segregating normal sized opaque kernels for the mutant alleles (-/-), and normal sized vitreous kernels for alleles (-/+ and +/+), with ratios of about 1:2:1, indicating the recessive nature of the causal mutation. The homozygous opaque seeds of rdm4 germinated normally and gave rise to morphologically normal seedlings. However, vegetative growth was slightly slower and adult plants were shorter, as shown at 2-week, 1-month, and adult stages (Fig. 1C-F). Male fertility was negatively affected such that only a few seeds were produced when plants were self-pollinated (Fig. 1G). Female fertility appeared to be normal as moderately wellfilled ears resulted from using other pollen sources.

The causal deletion that was initially annotated to contain three genes (GRMZM2G098603, GRMZM2G098596, and GRMZM2G176546) was mapped and identified previously by using BSEx-seq (Jia et al., 2018b). Here we re-estimated this deletion to be 5731 bp with genomic coordinates of two break points at 1 100 088 and 1 105 820 based on the B73 genome assembly v4, rather than 6248 bp previously estimated from the B73 v3 genome (Fig. 2). Two paired-end and 12 single-end reads in exome-seq, and the Sanger sequences of cloned PCR product with the primer pair of RDM4\_E5F and AMP\_E3R both covered this junction site and two break points (Fig. 2). The deletion actually contains only two predicted genes, an RDM4-like gene (Zm00001d023237) and an AMP-binding-like protein (Zm00001d023238). The opaque mutant phenotype results from loss of the RDM4-like gene (see confirmation below).

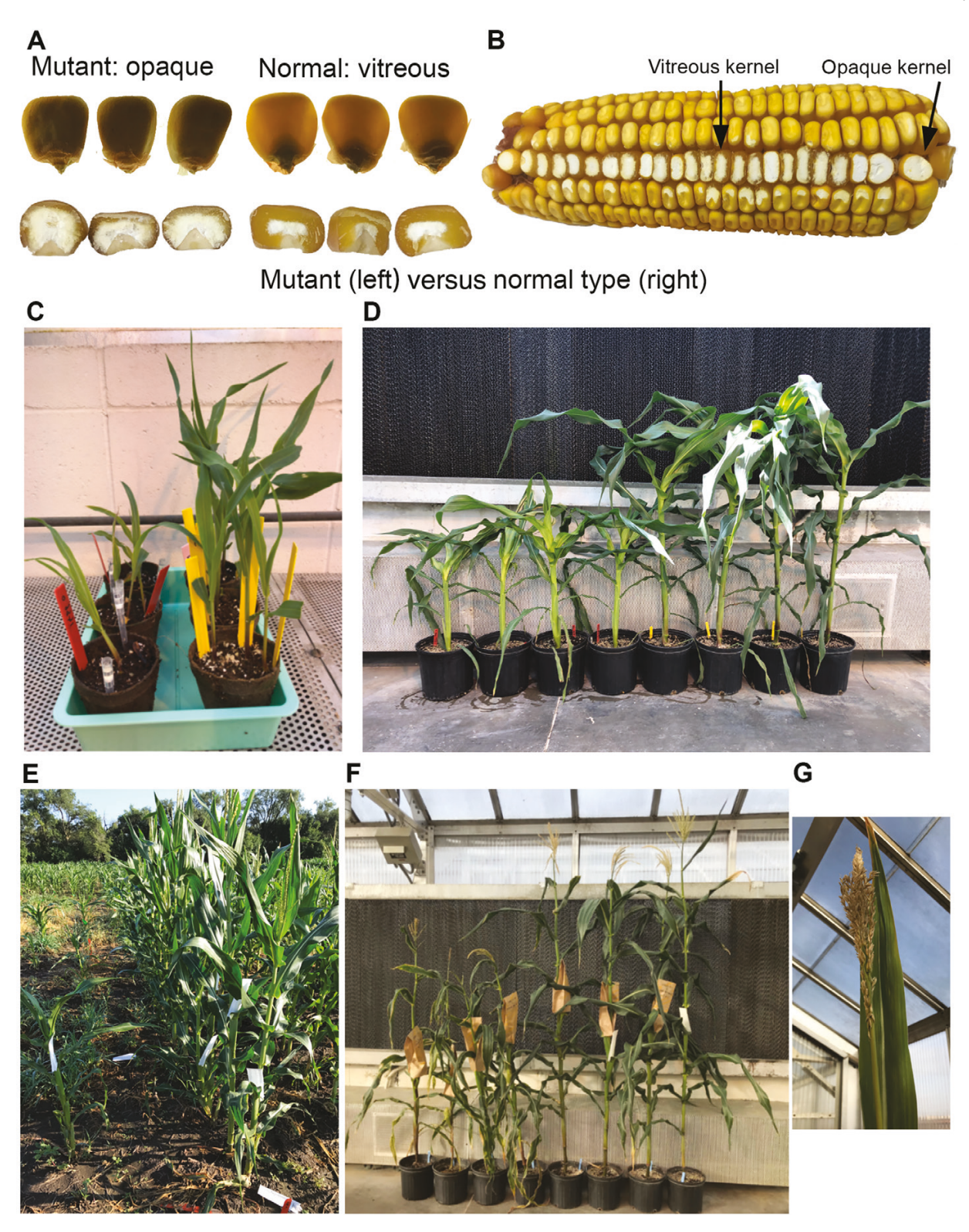
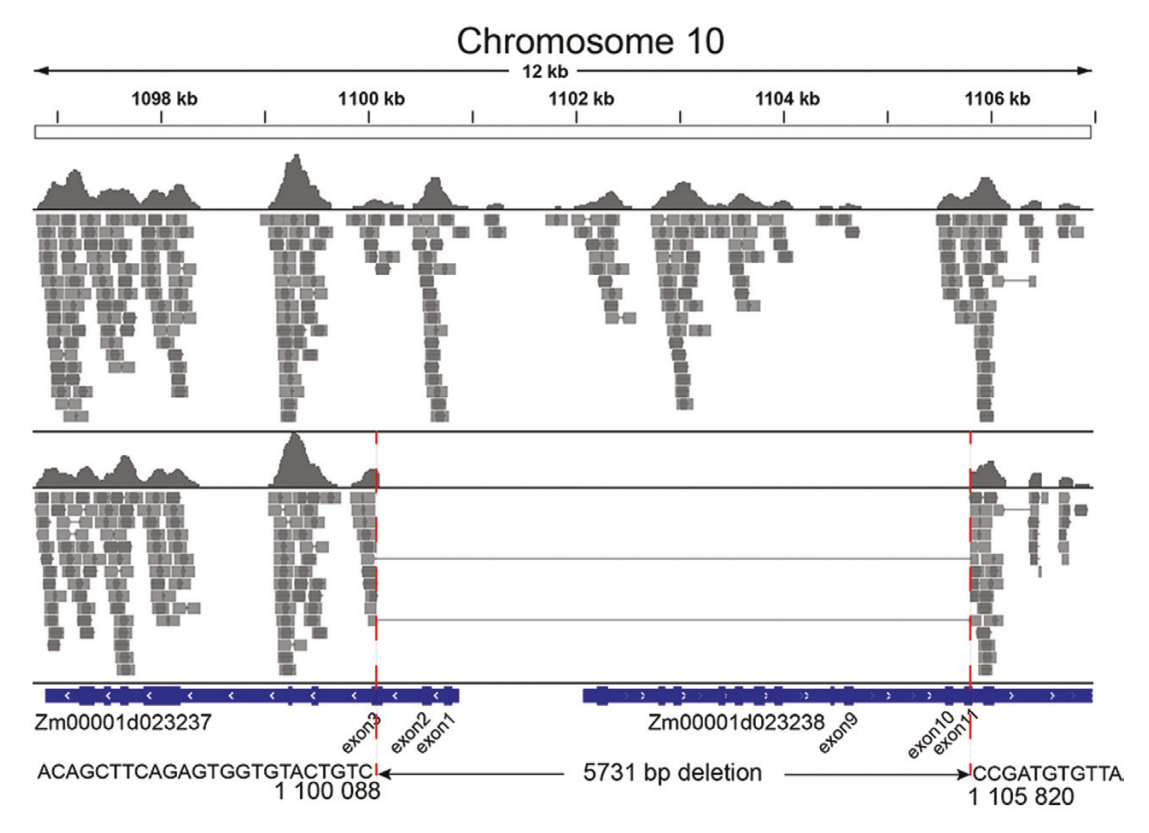


Fig. 1. Plant and kernel phenotype in B73 mutant rdm4. (A, B) Self-pollinated heterozygous F3 ear with segregation of opaque and vitreous kernels. (C) Mutant (left) and wild type/het (right) plants at 2 weeks after planting in the greenhouse. (D) Mutant (left) and wild type/het (right) plants at 2 weeks after planting in the greenhouse. (E) Mutant (left) and wild type/het (right) plants before pollination in the field. (F) Four mature mutant plants (left), four wild type/ het plants (right) in the greenhouse. (G) Sterile tassel in mutant plant.

# Confirmation of RDM4 as causal gene for opaque kernel and vegetative mutant phenotypes

To confirm the causal mutant gene in the deletion corresponding to opaque kernel and vegetative phenotypes, we obtained 10 UniformMU insertion lines in the two genes (see Supplementary Table S2). For all the UniformMU progeny, it was shown that mutations in the AMP-binding like gene had normal kernels and plants (Supplementary Fig. S1A) indicating that loss of this gene is not responsible for either phenotype. In contrast, segregation for opaque kernels was observed in



**Fig. 2.** Causal deletion covering *RDM4* gene in mutant *rdm4*. A deletion was identified exactly underneath the linkage peak by BSEx-seq, and covered the promoters and partial exons of two genes, Zm00001d023237 (*RDM4*) and Zm00001d023238. The deletion was determined to be of 5731 bp, with two joint sites' sequences shown, based on the cloning and sequencing of PCR product by primers (RDM4\_E5F and AMP\_E3R). (This figure is available in color at *JXB* online.)

the heterozygous UniformMU insertion lines for RDM4 gene. In the four UniformMU lines for RDM4, including UFMU000942 and UFMU06648, the received seeds and progeny seeds segregated for an opaque kernel phenotype similar to mutant rdm4 (Supplementary Fig. S1B, C) and opaque seeds gave rise to plants with reduced height like mutant rmd4 (Fig. 3). In the genotyped homozygous mutant plants for the lines of UFMU000942 and UFMU06648, the same vegetative phenotype was observed. For example, plant heights were significantly different between WT and mutant (Fig. 3B, C, E), and similar mutant plant heights were seen for UFMU000942 and rdm4 (Fig. 3D). The homozygous UFMU000942 and UFMU06648 mutant alleles produced almost sterile tassels (Fig. 3A), which was consistent with this phenotype in mutant rdm4. Finally, allelism test crosses between heterozygous rdm4 plants and the independent UniformMu alleles in UFMU00942 and UFMU06648 showed that these mutants fail to complement each other (Fig. 3F, G), and mutations in RDM4 cause the observed seed and vegetative phenotypes. RDM4 comprises 10 exons and nine introns, and encodes a protein containing 318 amino acid residues.

Zein reductions underlying opaque kernel phenotype and their effect on amino acid profiles

The opaque kernels in *rdm4* likely result from the striking reduction in zein storage proteins in an analogous way to *opaque-2* (Fig. 4A). However, zein protein and mRNA

expression analysis showed some key differences from o2. While the most striking effect in o2 was reduction of the 22 kDa α-zeins, in rdm4 the 19 kDa α-zeins gene families (Z1A, Z1B, and Z1D) were clearly more reduced than the 22 kDa  $\alpha$ -zeins (Z1C) at both the protein and the transcript level (Fig. 4A). This suggests that RDM4 may play a role in high-level mRNA expression of the extensively duplicated 19 kDa α-zein genes. Intriguingly, the O2 gene itself showed substantial reduction in expression (see Supplementary Fig. S2A, B), raising the possibility that RDM4 acts upstream of O2 in the endosperm mRNA expression hierarchy and may even play an overarching role in endosperm development. Unlike the opaque-2 mutant, which shows a substantial global increase in non-zein proteins, SDS-PAGE showed that such proteome rebalancing in rdm4 is not as pronounced as in o2 (Fig. 4B). Instead, rdm4 shows discrete increases and decreases of a few nonzein proteins (Jia et al., 2018b). Similar profiles of zein and non-zein proteins were observed in rdm4 deletion allele and UniformMU alleles (Fig. 4C, D). Heterozygous kernels had similar zein mRNA expression values as homozygous WT kernels in both RT-PCR and qRT-PCR, and this also applied to other related genes such as O1, O2, O10, OHP1, and OHP2 (Supplementary Fig. S2A, B). This slight and selective proteome rebalancing was reflected in an increase in protein-bound lysine (Lys, 1.4-fold, P<0.001) which is less than observed in the o2 mutant (2 fold, P < 0.001) (Table 1). The accumulation of most free amino acids was increased in

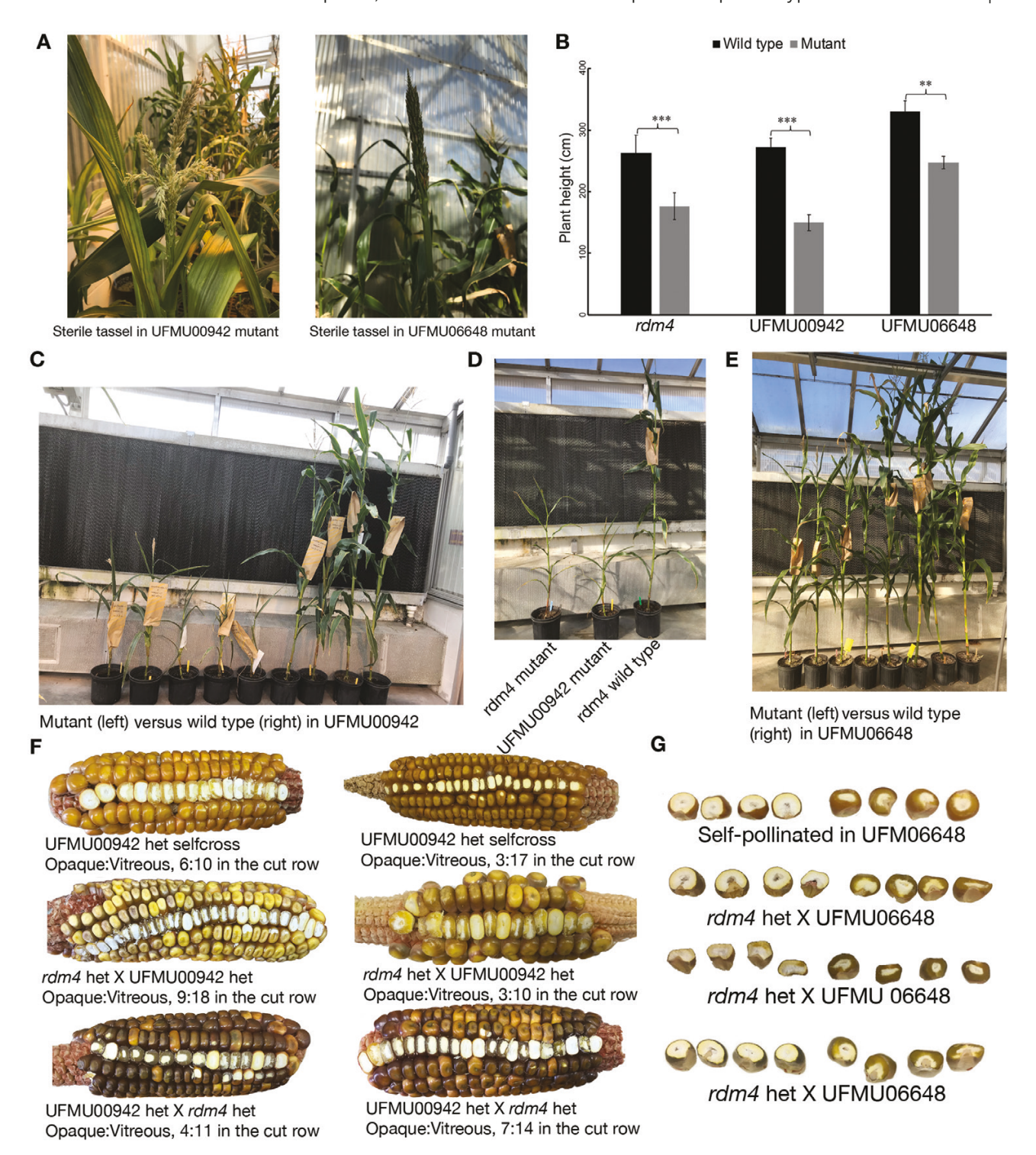


Fig. 3. Plant and kernel phenotype in UFMU lines and complementation test. (A) Sterile tassel in UFMU00942 and UFMU06648, same as in rdm4 mutant. (B) Significantly different plant height for wild type and mutant in the three lines, rdm4, UFMU00942, and UFMU06648. \*\*P<0.01, \*\*\*P<0.001. (C) Plant height for wild type and mutant in UFMU00942. (D) Comparison of mutant plant height between rdm4 and UFMU00942. (E) Plant height for wild type and mutant in UFMU06648. (F) Allelism test of heterozygous plants between rdm4 and UFMU00942. The heterozygous plants in UFMU00942 were self-pollinated and produced segregating ears with opaque and vitreous kernels. The reciprocal crosses of heterozygous plants between rdm4 and UFMU00942 produced the similarly segregating ears. (G) Allelism test of heterozygous plants between rdm4 and UFMU06648.

mature o2 seeds (average 3.3-fold increase across all amino acids; Table 1), which is likely a result of reduced zein synthesis and reduced incorporation into non-zein proteins. Mutant rdm4 seeds showed an even more profound increase in free amino acids in rdm4 (average 7.8-fold increase across all amino acids; Table 1), which likely reflects the general reduction in protein synthesis.

Proteomic and transcriptomic analysis of endosperm suggests radical disruption in mRNA expression and altered ability to rebalance the proteome

A shotgun proteome analysis involving 10-plex Tandem Mass Tag (TMT<sup>10</sup>) labeling of the non-zein proteins extracted from developing endosperm at 20 d after pollination (DAP) was

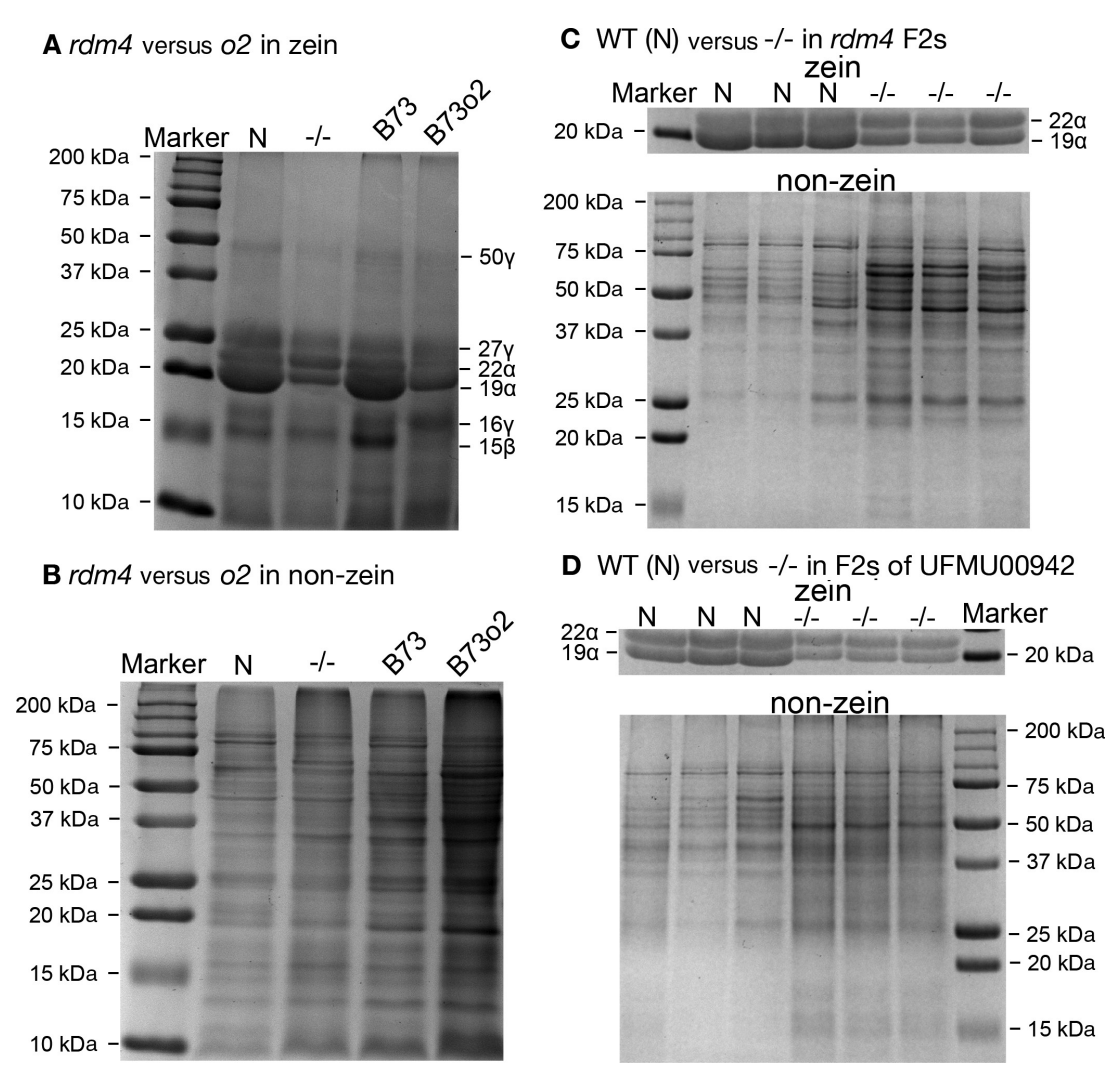


Fig. 4. Zein and non-zein SDS-PAGE in *rdm4* and UFMU lines. (A, B) Zein and non-zein proteins in a comparison of wild type (labeled as N) and mutant (as -/-) for *rdm4* and *B73o2*, which were published previously (Jia *et al.*, 2018b). (C, D) Zein and non-zein proteins in a comparison of vitreous kernel (labeled as N) and opaque kernel (as -/-) in *rdm4* and UFMU00942. Each lane represents the amount of zein or non-zein proteins based on the same amount of kernel flour (100 mg).

performed in both WT and rdm4 opaque mutants. Dissected embryos from these 20 DAP seeds were used for genotyping for homozygous opaque mutant and WT. The endosperm non-zein fraction was separated by LC-MS/MS. A total of 7675 proteins were confidently identified across all samples, including the four corresponding biological replicates. PCA was performed based on the protein abundance data, and biological replicates were denoted by a circle inclusion. The all-protein PCA could describe 75.1% of the explained variance in component 1 (PC1), and 9.8% in component 2 (PC2), totaling 84.9% of the explained variance.WT and the mutants could be separated spatially by PC1 (Fig. 5A).

We compared our proteomic data with that of the o2 mutant in our previously published work (Morton *et al.*, 2016), to identify commonalities and differences in rebalancing of the non-zein proteome. The proteomic analysis showed that the calculated lysine (abbreviated as K) content of the most abundant non-zein proteins (top 10 and top 20) in rdm4 and o2 was consistent with the measured lysine increase in Table 1, compared with WT (Fig. 6A). Lysine increase in the up-regulated non-zein proteins

was globally significant in rdm4 (see Supplementary Table S3), and less than that in o2. The amino acid content changes in rdm4 were very distinct from other opaque mutants (Morton et al., 2016). We compared the mutant and WT based on the abundance data, and produced 4075 and 303 DPs, respectively, in rdm4 versus WT and o2 versus WT (Table 2). It is not meaningful to draw inferences from the number of DPs in rdm4 compared with that of o2. This is because the proteomic data in the two mutants were collected using two different methodologies. However, we can compare the relative number of increased and decreased proteins in each mutant. A higher proportion of DPs were decreased in o2 (61.39%) than in rdm4 (51.04%). Given that the SDS-PAGE (Fig 4B) clearly showed that proteome rebalancing was different in o2 compared with rdm4, it is likely that the highly abundant proteins visible on the SDS-PAGE and contributing to the general increase in the non-zein proteome in o2 are among the 38.61%. The fold changes of both increased and decreased DPs appeared to be greater, on average, in o2 than in rdm4, as indicated by more green and red dots further away from the zero axis in Fig. 6B. We also calculated the size of the

Table 1. Amino acid content in rdm4 and B73 o2

	4	æ	z	۵	A R N D N/D Q	ø	ш	Q/E G		I	_	_	¥	Σ	ш	۵	S	*	<b>-</b>	>	>	C	All aa
Free aa																							
B73o2/Normal	3.3	3.3 0.3 1.3 10.4	1.3	10.4		7.1	3.2		2.9	2.8	က	2.2	1.7	2.2	3.2	က	2.7	က	2	9			ω <u>.</u>
B73rdm4/Normal	9.9	9	1.9	7		18.4	4.6		8.6	3.6	7.9	15.4	1.6	8.6	11.3	4.9		~	14.5	5.8	11.7	2.1 7.	7.8
PB aa																							
B73o2/Normal	0.8 1.7	1.7			1.7			8.0	_	<del>د</del> .	6.0	0.7	2	0.7	6.0	8.0	_		_	0.8	1.2	_	Ψ.
B73rdm4/Normal 0.8 1.1	0.8	1.			1.4			0.8	0.8	6.0	0.8	0.7	4.1	<del></del>	2.0	0.7	8.0		6.0	0.7	_	0	6.0
							:		:														

Relative free and protein-bound (PB) amino acid fold increases (more than 1) or decreases (less than 1) in mature kernel flour from B73 opaque-2 and B73 rdm4 mutants compared with normal sibling kernels. Ratios were calculated from average % (w/w) amino acid against kernel flour from four biological replicates (data not shown). In PB amino acids, N/D represents asparagine/aspartic acid, Q/E represents glutamine/glutamic acid, and W (tryptophan) and C (cysteine) were not detected with the acid hydrolysis used. 'All aa' is the average change across all detected amino acids.

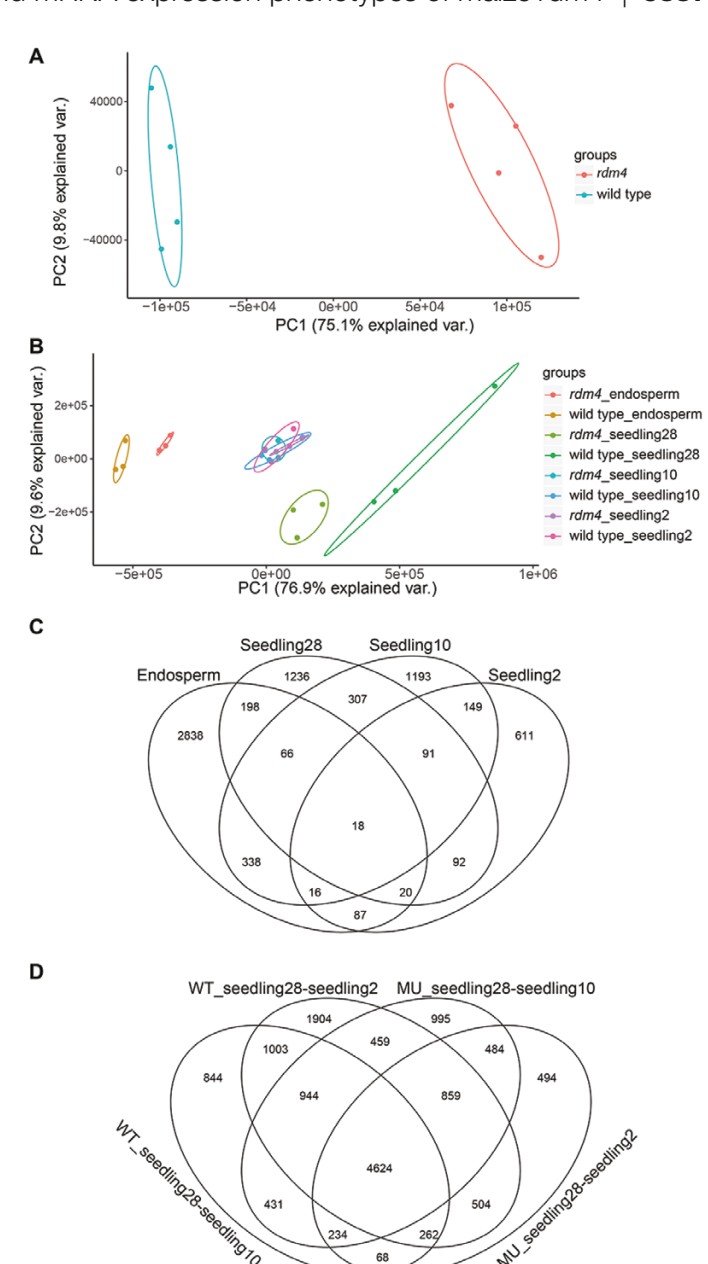
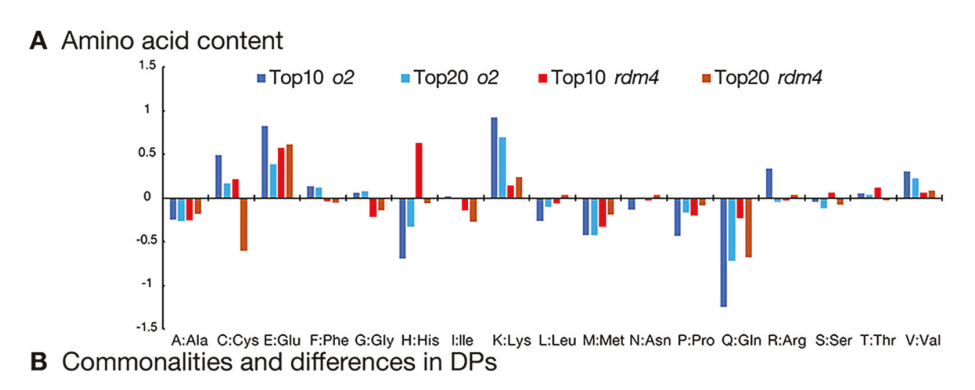
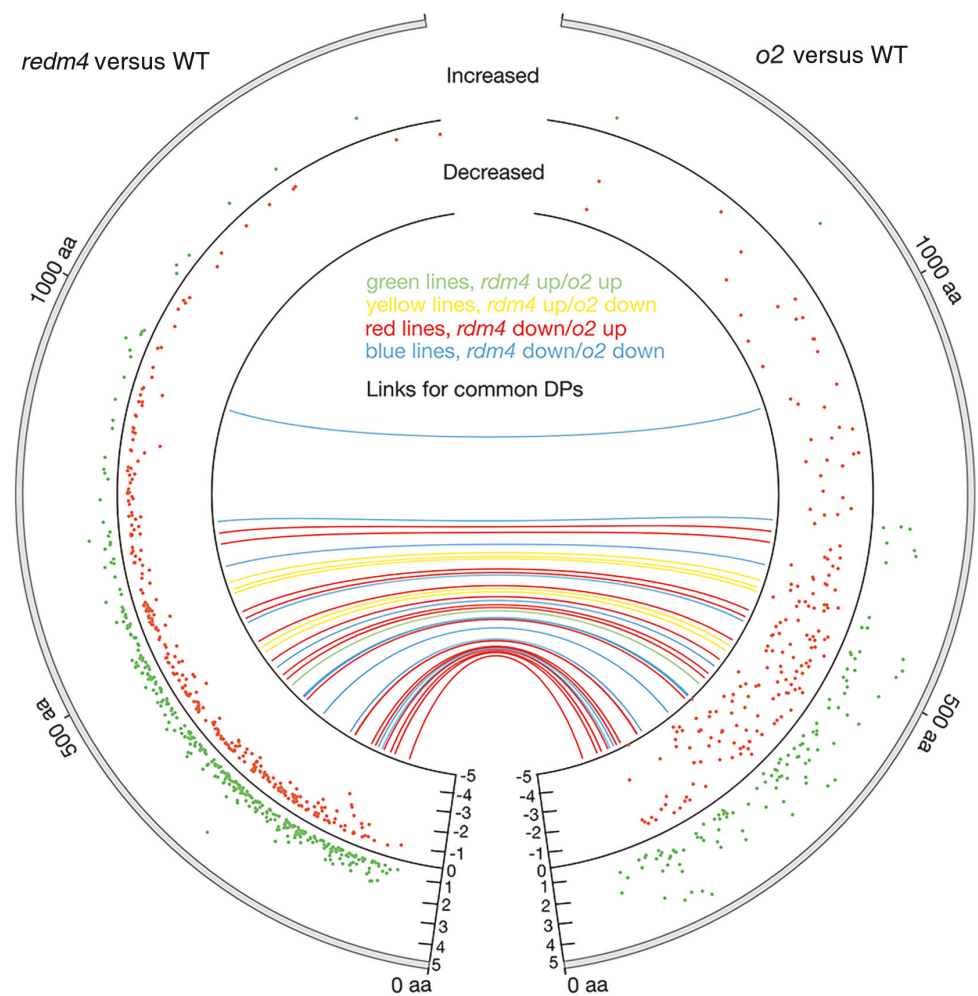


Fig. 5. Principal component analysis (PCA) and Venn diagram in analysis of proteomics and RNA-seq data. (A) PCA plotting for proteomic analysis conducted in endosperm. (B) PCA plotting for RNA-seg analysis conducted in endosperm and leaf. (C) Venn diagram of DEGs in endosperm, seedling28, seedling10, and seedling2. (D) Venn diagram of cold responsive DEGs in wild type and rdm4 mutant. The differentially expressed genes were achieved between the pairs wild type leaves seedling28 and seedling10, wild type leaves seedling28 and seedling2, rdm4 mutant (MU) leaves seedling28 and seedling10, and rdm4 mutant leaves seedling28 and seedling2.

DPs (P<0.05) whose peptide sequences were downloaded from the Uniprot database in the two mutants and showed a difference of fold change of the increased (green dots in Fig. 6B) and decreased (red dots in Fig. 6B) proteins between o2 and rdm4 over their length distribution. It is likely that some of the commonly increased or decreased proteins in rdm4 and o2, as well as common proteins with opposite trends, were visible as differential bands in the SDS-PAGE gels of non-zein proteins in rdm4 and o2 (Fig. 4B). Of the DPs (P<0.05 and |log2(fold





**Fig. 6.** Commonalities and differences of amino acid content and DPs in *rdm4* and *o2*. (A) Amino acid content was calculated for the top 10 and 20 significant increased and decreased non-zein proteins in proteomic analysis, compared with WT. (B) The DPs' length based on the amino acid counts was calculated and plotted for *rdm4* versus WT and *o2* versus WT. Color code, green and red dots for scatter plotting of |log2(fold change)| >0.5 of increased (positive) and decreased (negative) DPs (*P*<0.05), respectively; green, yellow, red and blue lines for the common proteins of *rdm4* up/o2 up (green), *rdm4* up/o2 down (yellow), *rdm4* down/o2 up (red), and *rdm4* down/o2 down (blue), respectively, in the two mutants. The outer layer indicates the amino acid number for protein size.

Table 2. Summary of DPs in rdm4 and o2 compared with WT

ruma versus vvi	o2 versus WT
4075	303
48.96%	38.61%
51.04%	61.39%
	48.96%

DPs were based on P<0.05 in the proteomic analysis.

change)  $|>0.5\rangle$  found in rdm4 from the proteomics, 37 of these were also among the DPs found in o2 although some of them were opposite in their increase or decrease between the two

mutants. The DPs accordingly separated into four groups. One protein was increased in both rdm4 and o2 (green colored line in Fig. 6B), five proteins were increased in rdm4 and decreased in o2 (yellow colored line in Fig. 6B), 17 proteins were decreased in rdm4 and increased in o2 (red colored line in Fig. 6B), and 14 proteins were decreased in both rdm4 and o2 (blue colored line in Fig. 6B). For example, elongation factor  $1-\alpha$  (B6TWN7) as an indicator of protein synthesis was increased and decreased in rdm4 and o2, respectively (Table 3). These differences suggest that proteome rebalancing of non-zein proteins in the two mutants is quite distinct. Interestingly, we found proteins

with different regulation patterns in subcellular locations. Of the 98 DPs (P<0.05, fold change>2), 51 and 47 DPs were significantly increased and decreased, respectively (Supplementary Table S3). It is notable that for subcellular location, 18 out of 51 increased DPs predicted were predicted to be nuclear localized, while all the 47 down-regulated DPs were predicted to be non-nuclear localized, based on the search in the UniProt website. We identified 50 kDa and 27 kDa γ-zeins decreased in the list of most significant DPs (Supplementary Table S3). γ-Zeins are known to partially fractionate with non-zein proteins, unlike the hydrophobic  $\alpha$ -zeins. The enrichment analysis of DPs on the STRING website showed that the increased DPs were enriched in the KEGG pathway of 'ribosome biogenesis', while the decreased DPs were enriched in 'plant hormone signal transduction'.

Endosperm RNA-seq analysis in WT versus rdm4 was used to test whether they were consistent with the protein abundances in the mutant versus WT. Of the 51 increased DPs (see Supplementary Table S3), 46 of the corresponding transcripts were with fold change >1, and 39 transcripts were significant (P<0.05). Of the 47 decreased DPs, 41 of the corresponding transcripts were with fold change <1, 18 of which were significant. For example, elongation factor  $1-\alpha$ (Uniprot ID: B6TWN7; Gene ID: Zm00001d021788) and rRNA methyltransferase (Uniprot ID: A0A1D6FKG8; Gene ID: Zm00001d009597) as indicators of protein synthesis were increased with a consistency in protein and transcript abundance, as was histone 2B (Uniprot ID: B4FZO6: Gene ID: Zm00001d005789). Down-regulated corresponding genes were also significantly differentially abundant between WT and mutant in RNA-seq. For example, the transcript abundance of granule-bound starch synthase (Uniprot ID: Q5NKP6; Gene ID: Zm00001d033937) also corresponded to a protein decrease.

**Table 3.** DPs in *rdm4* and *o2* mutants compared with WT

Group	Uniprot	rdm4 versu	s wt	o2 versus w	rt	Gene description
		Log2(FC)	P	Log2(FC)	P	
rdm4 up, o2 up	B4FYA8	0.62	1.50×10 <sup>-20</sup>	2.6	0.0375	Tyrosine specific protein phosphatase-like
rdm4 up, o2 down	A0A1D6LZP3	0.65	1.40×10 <sup>-5</sup>	-1.25	0.0041	Alliin Iyase
	B6TWN7	1.72	4.20×10 <sup>-71</sup>	-0.63	0.0076	Elongation factor 1-α
	C0P5B0	0.56	2.80×10 <sup>-15</sup>	-2.98	0.0006	Asparaginyl-tRNA synthetase
	C4JC17	0.73	2.70×10 <sup>-23</sup>	-3.56	0.0203	H/ACA ribonucleoprotein complex subunit
	K7VIA0	0.67	9.30×10 <sup>-21</sup>	-1.53	0.01	Homolog of nucleolar protein NOP56
rdm4 down, o2 up	A0A1D6E987	-0.59	2.30×10 <sup>-3</sup>	3.6	0.0127	Galactose mutarotase-like
	A0A1D6G9W0	-1.1	5.55×10 <sup>-17</sup>	0.92	0.0191	Seed storage 2S albumin superfamily prote
	A0A1D6JST8	-0.6	5.20×10 <sup>-20</sup>	3.5	0.0448	β-Glucosidase 40
	A0A1D6KR27	-0.52	4.06×10 <sup>-11</sup>	1.25	0.01	Prolyl carboxypeptidase like protein
	A0A1D6L4E9	-0.53	$2.41 \times 10^{-19}$	1.05	0.048	Exoglucanase1
	A0A1D6L4F0	-0.89	2.80×10 <sup>-8</sup>	2.51	0.0196	Exhydrolase II
	A0A1D6MSG1	-1.22	9.30×10 <sup>-119</sup>	3.69	0.0336	α-L-Fucosidase 2
	A0A1D6NE76	-0.87	2.40×10 <sup>-6</sup>	3.3	0.0408	Cytidine deaminase
	A0A1X7YIL8	-0.85	4.78×10 <sup>-76</sup>	0.8	0.0097	FAS1 domain-containing protein
	B4FGM4	-0.53	2.42×10 <sup>-27</sup>	1.17	0.0169	Endothelial differentiation-related factor 1
	B4FZU9	-0.79	2.80×10 <sup>-30</sup>	1.2	0.0248	Dihydropyrimidine dehydrogenase (NADP)
	B6SHW9	-0.54	1.80×10 <sup>-5</sup>	0.85	0.0007	Ubiquitin fusion protein
	B6SI37	-1.61	8.20×10 <sup>-27</sup>	1.15	0.0138	Embryo specific protein1
	B6TFN1	-0.61	1.10×10 <sup>-04</sup>	1.14	0.0088	NAD(P)H dehydrogenase (quinone) FQR1
	B6TN41	-0.52	3.26×10 <sup>-9</sup>	1.26	0.006	4-Hydroxy-4-methyl-2-oxoglutarate aldolas
	P19656	-0.94	6.70×10 <sup>-3</sup>	0.85	0.0143	Non-specific lipid-transfer protein
	Q29SB6	-0.57	2.50×10 <sup>-9</sup>	1.37	0.0008	Pathogenesis-related protein 10
rdm4 down, o2 down	A0A1D6GAK2	-0.76	2.00×10 <sup>-94</sup>	-3.56	0.0243	Signal recognition particle 54 kDa protein 3
	A0A1D6LH71	-0.63	$8.00 \times 10^{-14}$	-2.63	0.0408	Mannose-specific jacalin-related lectin
	A0A1D6N7J6	-0.54	0.0113	-0.99	0.0114	Osmotin-like protein
	B4F939	-0.51	2.67×10 <sup>-24</sup>	-3.02	0.0276	Histone deacetylase
	B4FM15	-0.5	8.30×10 <sup>-27</sup>	-1.08	0.0265	60S ribosomal protein L28-1
	B4FX24	-0.65	4.80×10 <sup>-5</sup>	-4.28	0.0019	Mitochondrial outer membrane protein pori
	B6SQM0	-0.73	1.40×10 <sup>-15</sup>	-3.29	0.0377	Major pollen allergen Car b 1 isoforms
	B6TB84	-0.66	5.80×10 <sup>-4</sup>	-0.9	0.0234	Soluble inorganic pyrophosphatase 1
	C0HFQ1	-0.66	1.10×10 <sup>-12</sup>	-3.65	0.0046	Mannose-specific jacalin-related lectin
	C0P3N8	-0.51	$4.41 \times 10^{-13}$	-2.63	0.0011	Indole-3-acetic acid-amido synthetase
	C0PDC7	-0.62	1.40×10 <sup>-11</sup>	-1.01	0.0181	Chaperone protein ClpB1
	COPDX9	-0.7	5.90×10 <sup>-7</sup>	-4.96	0.0001	Mannose-specific jacalin-related lectin
	K7TFF5	-0.77	7.20×10 <sup>-11</sup>	-3.51	0.0073	Defective18
	Q6XZ79	-0.99	4.40×10 <sup>-45</sup>	-2.61	0.0007	Fructokinase-1

DPs are selected with P<0.05 and |log2(fold change)| >0.5 in the proteomic analysis.

The 20-DAP endosperm RNA-seq analysis was used to glean clues as to the function of RDM4 in endosperm. Genotyping using embryo DNA was used to identify homozygous mutant and WT alleles. Based on genotyping results, endosperm tissue was used for RNA extraction for RNAseq. The three replicates of WT and mutant were grouped well by PC1 in the PCA (Fig. 5B). As expected, the RDM4 (Zm00001d023237) transcript was not detected in the mutant, while it was in abundance in WT. In total, 3581 DEGs, including 2022 up-regulated and 1559 down-regulated transcripts, were found significant (P<0.05) between WT and mutant (see Supplementary Table S4). More than 80 down-regulated DEGs were annotated as transcription factors, including O2 (Zm00001d018971), and zein genes were comprehensively down-regulated, including 50 kDa γ-zein (Zm00001d020591), 19 kDa zein (Zm00001d048848, Zm00001d030855, Zm00001d048847, Zm00001d048849, Zm00001d048850, Zm00001d048851, Zm00001d048852), 22 kDa α-zein (Zm00001d048806 and Zm00001d048807), and 16 kDa zein (Zm00001d005793). These were consistent with RT-PCR results (Supplementary Fig. S2). In addition, >109 transcription factors were up-regulated. These results suggest that developing endosperm zein and non-zein mRNA expression profiles were significantly influenced by the loss of RDM4. To identify the key pathways affected, the fold-change values of 1500 DEGs (P<0.001) for endosperm were subjected to a Wilcoxon bin-wise statistical test and plotted in MapMan (Supplementary Fig. S3). This showed a pathway enrichment, including an increase of protein biosynthesis (especially ribosome biogenesis) and histones in endosperm of rdm4, and a decrease of components of RdDM, vesicle trafficking, solute transport, redox homeostasis, ethylene biosynthesis, lipid metabolism, starch metabolism, and protein modification.

# Transcriptional changes in leaves in response to cold stress

Given the evidence that RDM4 plays a role in mediating cold stress in Arabidopsis (Chan et al., 2016), we addressed whether transcript profiles suggest it might play a similar role in maize stress responses. While RDM4 is equally likely to play a broader role in stress responsiveness, we focused on cold for the above reason. We investigated the transcriptomic changes resulting from the loss of RDM4 in maize vegetative development in normal (28 °C, 16 h day, 8 h night for 14 d; seedling28), mild cold stress (28 °C for 11 d followed by 10 °C for 3 d; seedling10) and near freezing severe cold stress (28 °C for 11 d, 10 °C for 3 d followed by 2 °C for 1 d; seedling2) conditions. Rdm4 mutant plants were visibly less healthy than WT after 3 d at 10 °C (seedling10), exhibiting significant leaf necrosis. Similarly, WT plants were obviously more resistant to severe cold stress (seedling2) since their leaves were less necrotic than those of mutant plants (see Supplementary Fig. S4A, B). Transcriptomic analysis in leaf tissue confirmed that the expression of RDM4 was absent in the mutant as expected. A different transcript pattern was observed in seedling28 of rdm4 mutant, with 848 up- and 1180 down-regulated DEGs between WT and mutant (Supplementary Table S4). The

pathways of photosynthesis, nutrient uptake, cell cycle organization, and redox homeostasis were impaired in seedling28 of *rdm4* mutant, while lipid metabolism, protein biosynthesis and modification, cell wall organization, and chromatin organization were enhanced (Supplementary Fig. S3).

The RNA-seq analysis identified extensive changes in transcriptome for response to mild and severe cold stresses that appeared to be independent of RDM4. Cold stress (seedling10 and seedling2) separated the samples from seedling28 based on the transcripts in RNA-seq (Fig. 5B) and resulted in up-/ down-regulated DEGs, with 1329/849 and 345/739 for seedling10 and seedling2, respectively (see Supplementary Table S4). Based on the transcriptome data, we identified tissuespecific expression in endosperm and leaf (Fig. 5C), and found only 18 transcripts were all significantly changed in the four comparisons of mutant versus WT in endosperm, seedling28, seedling10 and seedling2 (Table 4). A spearman correlation between RDM4 and all the other genes was calculated across all the 18 seedling samples, and the significance was assessed by using Student's t-test. In total, 1306 genes with significant P values (P<0.05) for correlation coefficient were observed. In this way, we identified five genes significantly positively correlated to RDM4 (Table 4). In the same way, 29 DEGs (P<0.01) in the three pair-wise comparisons for seedling leaf were shown with significant correlation values (P<0.05), including 13 genes negatively correlated and 16 genes positively correlated (Supplementary Table S5).

To dissect the possible contribution of RDM4 to the response to cold stress in the seedlings of rdm4 mutants, we conducted four pairwise comparisons of transcriptomic expression, i.e. in WT leaves between seedling28 and seedling10 (for the DEGs by both RDM4 and cold stress) and between seedling28 and seedling2 (for the DEGs by both RDM4 and cold stress), in rdm4 mutant leaves between seedling28 and seedling10 (for the DEGs by only cold stress) and between seedling28 and seedling2 (for the DEGs by only cold stress). In the Venn diagram, 4624 DEGs overlapped in the four comparisons (Fig. 5D, Supplementary Table S4), and they contributed to response to cold stress, but their regulation was not directly related to RDM4. We observed some DEGs apparently related to RDM4. There were 8410 and 10 559 DEGs in a comparison of seedling28 versus seedling10 and seedling28 versus seedling2, respectively in WT. Of these, 2177 (25.9%) genes were not differentially expressed in rdm4 mutant (WT seedling28-seedling10 versus mutant (MU) seedling28-seedling10, i.e. 1003 + 844 + 68 + 262 = 2177 in Fig. 5D). Near freezing treatment for seedling2 induced more genes with a potential regulation of RDM4, as 4310 (40.8%) genes were not found in WT seedling28-seedling2 versus MU seedling28-seedling2, i.e. 1904 + 1003 + 459 + 944 = 4310 (Fig. 5D). This suggested that the loss of RDM4 caused a subset of cold-stress-responsive genes to lose responsiveness to cold. This subset was larger in the more severe cold stress.

Of the large group of DEGs with a potential regulation of RDM4, we selected a subset of representative genes whose cold-induced transcript expression was not observed or was much less pronounced in *rdm4* leaves to conduct a real time qRT-PCR analysis. The results supported that *RDM4* may

Table 4. Genes significantly correlated with RDM4 in all the endosperm and seedling samples

	Correlati coefficie		Fold change <sup>b</sup>				
	All	SE	EN	S28 <sup>b</sup>	S10 <sup>b</sup>	S2 <sup>b</sup>	Annotation
Zm00001d023237	1***	1***	160***	400**	900***	360**	RDM4
Zm00001d023238	0.92***	0.89***	49.95***	6700***	8460***	5050***	AMP-binding-like protein
ENSRNA049477092	0.85***	0.78***	9.48***	7.27***	3.96***	3.29***	Plant_SRP
Zm00001d038302	0.73***	0.81***	5.94***	11.93***	400**	280**	ROS1
Zm00001d044267	0.53**	0.77***	5.3***	5.54***	3.71***	2.72***	Glyoxylate/succinic semialdehyde reductase 2
Zm00001d037700	0.45*	0.78***	2.22***	1.49**	1.37*	1.55*	Heat shock 70 kDa protein
Zm00001d032298	0.2	0.61**	3.31*	1.57**	1.54**	1.64*	Trehalose-6-phosphate phosphatase1
Zm00001d015376	0.16	0.79***	0.62***	1.28*	1.4**	1.57***	Phosphoglycerate kinase
Zm00001d044686	0.16	0.5*	13.28***	1.9***	1.42**	1.89**	Phospholipid transfer protein homolog2
Zm00001d036768	0.04	0.14	0.49*	3.79*	0.53**	2.55**	MYB-transcription factor 158
Zm00001d031908	0.04	0.52*	0.61**	1.63***	1.38**	1.39*	Superoxide dismutase, SOD
Zm00001d023929	-0.06	0.33	0.41***	1.72***	1.48**	1.36*	Oxo-glutarate/malate transporter1, ZmpOMT1
Zm00001d027329	-0.12	-0.69*	1.53**	0.58**	0.55**	0.43*	DNA (cytosine-5)-methyltransferase DRM2
Zm00001d005315	-0.24	0.02	0.52*	0.62*	0.57***	1.71*	Calcium-dependent lipid-binding (CaLB domain) family protein
GRMZM5G884707	-0.3	-0.84***	0.64*	0.53***	0.68***	0.57***	Cytochrome b, COB
Zm00001d024583	-0.39	-0.35	0.63**	0.4***	0.58***	0.6**	DNA-directed RNA polymerase II subunit 1, NRPB1
Zm00001d007287	-0.48**	-0.78***	0.07***	0.04***	0.04***	0.08***	60S ribosomal protein L18a-2
Zm00001d029394	-0.63***	-0.77***	0.55***	0.62***	0.54***	0.6**	Histone H3

<sup>&</sup>lt;sup>a</sup> Correlation coefficient values were calculated for RDM4 and other genes' expression in all the 24 samples of endosperm and seedling (All), and the 18 samples of seedling (SE).

play an overarching role in coordinating transcriptional responses to cold (Fig. 7; Supplementary Fig. S5). RDM4 was induced by cold stress in WT (Fig. 7A). Based on the expression pattern shaped by a loss of RDM4 and cold stress, we observed four expression patterns. First, some genes' expression was increased in rdm4 mutant at 28 °C but not increased in rdm4 in response to cold (see the left panel in Fig. 7B-E; Supplementary Fig. S5A-L), which indicated a loss or alleviated repression in WT in cold stress and was consistent with RNA-seq results. We observed strong induction in response to cold (10 °C and/or 2 °C) in WT, but a similar cold induction is either substantially reduced or absent in rdm4 mutant (see the right panel in Fig. 7B-E; Supplementary Fig. S5A-L). Second, transcript expression of DNA-directed RNA polymerase II subunit 1 (NUCLEAR RNA POLYMERASE B1, i.e. NRPB1, Zm00001d024583) and histone 3 was unchanged or slightly increased in rdm4 mutant at all temperatures, and cold-induced expression changes in WT were similar in rdm4 mutant (Fig. 7F, G), as well as methyl transferase (Zm00001d027329) and auxin transcription factor (Zm00001d018414) (see Supplementary Fig. S5M, N). Third, expression of jasmonate methyltransferase (Zm00001d052827) was impaired in rdm4 mutants, and cold stress also contributed to its expression changes (Fig. 7H), which is consistent with the correlation results (see Supplementary Table S5). Fourth, conversely, the expression of cytokinin riboside (Zm00001d038862) and 60S ribosomal protein (Zm00001d007287) was significantly increased in rdm4 mutant at all temperatures, and we found strong induction in response to cold in WT, but a lesser response to cold in rdm4 mutant (Fig. 7I, J).

# **Discussion**

RDM4 plays a general role in the seed proteome and the mutant shows altered proteome rebalancing compared with o2

When the expression of zein storage proteins is interrupted by loss of regulatory factors such as opaque-2, compensatory mechanisms result in the increase of non-zein proteins and relatively constant levels of total proteins in maize seeds. This compensatory shift has been referred to as 'proteome rebalancing' (Holding, 2014; Wu and Messing, 2014; Li and Song, 2020). Proteome rebalancing has also been observed in sorghum (da Silva et al., 2011), rice (Kawakatsu et al., 2010; Takaiwa et al., 2018) and soybean (Schmidt and Herman, 2008).

Vegetative phenotypes were reported in the Arabidopsis mutant for RDM4/DEFECTIVE IN MERISTEM SILENCING 4 (DMS4) (He et al., 2009; Kanno et al., 2010) and no mention was made of a role in seed storage proteins. In the maize rdm4 mutant, similar vegetative phenotypes were accompanied by an opaque kernel phenotype resulting from reduced zeins and the resultant proteome rebalancing led to altered amino acid profiles (Table 1; Fig. 6A). Loss of RDM4 function substantially changes the endosperm transcriptome and proteome, although it is not yet known the extent to which RDM4 is directly and indirectly involved in regulatory processes. The decrease in zeins and increase in non-zeins (proteome rebalancing) were shown in rdm4 reflected by a proteome that was completely different from WT, and supported by RNA-seq data. The classical mutant opaque-2 has long been known to increase kernel lysine content through reduced accumulation of zeins and a compensatory increase in non-zeins and this results from the

<sup>&</sup>lt;sup>b</sup> Fold changes (WT/rdm4) are listed for endosperm (EN), and all the three seedlings (S28, seedling28; S10, seedling10; S2, seedling2).

<sup>\*</sup>P<0.05. \*\*P<0.01. \*\*\*P<0.001.

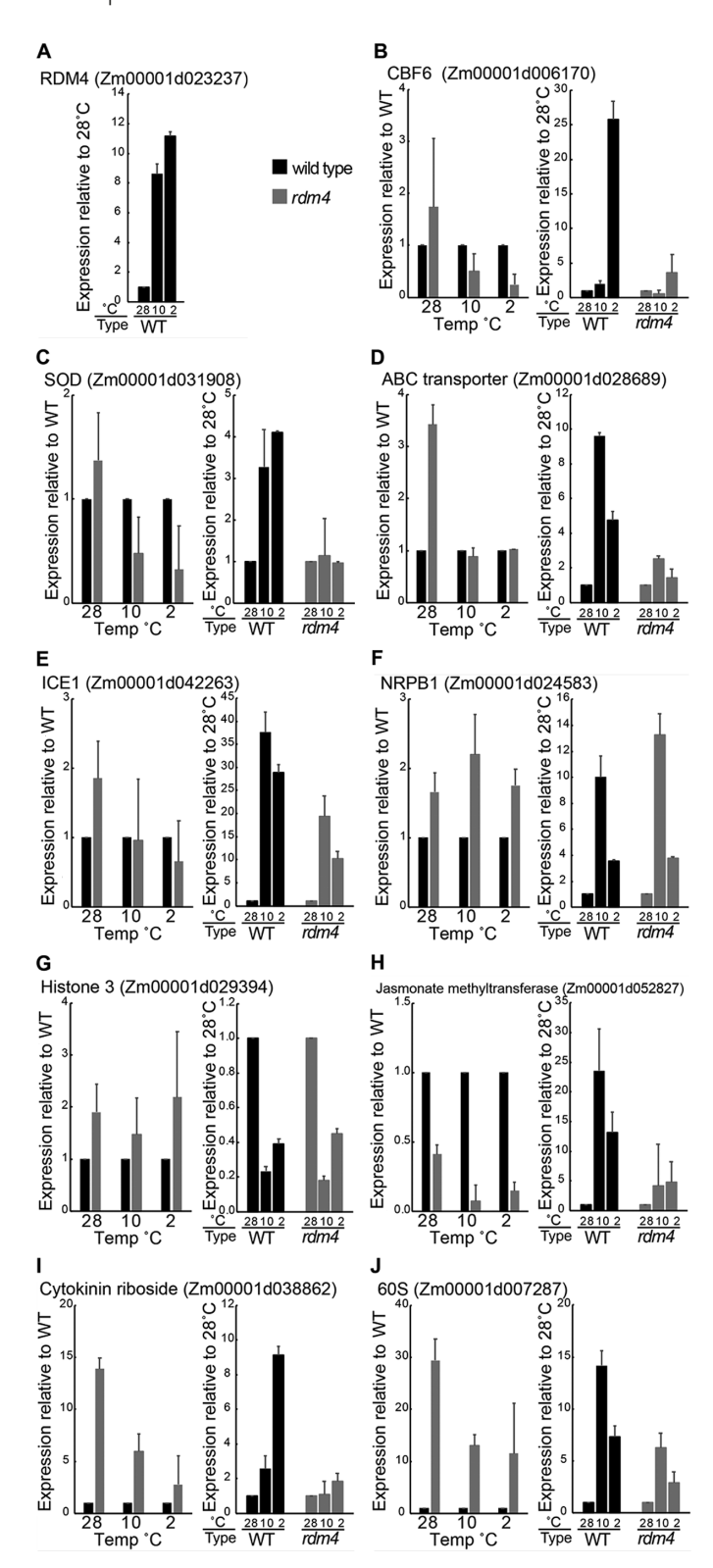


**Fig. 7.** The results of qRT-PCR for candidate genes regulated by *RDM4* in response to cold stress in seedlings. Relative expression of each gene is shown in two ways, which are differently informative. The first way (left panel of each graph) calculates the mRNA expression in *rdm4* mutant relative to wild type for each temperature. The second way (right panel) calculates expression for wild type and *rdm4* mutant separately, as a response to cold, compared with their respective expression at 28 °C. (A) The *RDM4* expression was induced by cold stress at 10 °C and 2 °C. (B, C, D, E) The left graphs show that expression of the four genes was increased in *rdm4* mutant at 28 °C but not increased in *rdm4* in response

loss the multi-function O2 transcription factor (Moro et al., 1996; Holding and Larkins, 2006). Although rdm4 also shows generally reduced zeins, the SDS-PAGE comparison shows that the increase in non-zein proteins is not as pronounced as that of o2. This may reflect a more generalized and overarching role for RDM4 than for O2 in the endosperm proteome. We therefore compared the proteome changes of WT:rdm4 to that of WT:02. Although the two proteomic datasets were derived from different methodological platforms that yielded very different total numbers of DPs, we were able to identify proteins that were either commonly increased or commonly decreased or showed opposite trends between rdm4 and o2 (Fig. 6B). Interestingly, comparison of the data sets suggested higher fold changes of DPs in o2 than in rdm4, which might suggest that a relative high abundance of the minority fraction of nonzein proteins in o2 made the most substantial contribution to the visible bands on SDS-PAGE gels (Fig. 4B). The generally higher fold changes in DPs in o2 than in rdm4 is consistent with O2 being required for expression of only a subset of genes expressed in the endosperm while RDM4 likely contributes to the transcriptional apparatus in a more general sense and for a greater fraction of genes expressed in the endosperm. Overall, these results suggest that proteome rebalancing is a complicated process likely affected by multiple levels of regulation.

It is known that zein accumulation accounts for almost a half of storage proteins in maize, but zeins lack lysine and tryptophan (Holding, 2014). The proteome analysis of o2 mutant indicated that some lysine-rich proteins, such as sorbitol dehydrogenase and glyceraldehyde-3-phosphate dehydrogenase, had increased abundance in mature kernels of o2 mutant (Jia et al., 2013). Since the rdm4 mutant displays negative and pleiotropic vegetative and reproductive phenotypes that would preclude its use as a source of increased lysine grain, we were nonetheless interested to understand the basis of its increased kernel lysine. We used proteomic data to evaluate both increased and decreased proteins on the amino acid content, and found that the in silico-calculated lysine content was increased in the top 10 and top 20 most abundant proteins (Fig. 6A) and in most of the significant up-regulated proteins (see Supplementary Table S3). The results explained the lysine increase by the DPs, which were not the same proteins as those causing the lysine increase in o2. For example, elongation

to cold. The right graphs show strong induction of the genes in response to cold (10 °C and/or 2 °C) in wild type, but a similar cold induction is either substantially reduced or absent in *rdm4* mutant. (F, G) The left graphs show that expression of the two genes was slightly increased in *rdm4* mutant at all temperatures. The right graphs show that cold induced expression changes in wild type (increases or decreases) are similar in *rdm4* mutant suggesting regulation of this gene by cold stress is independent of RDM function. (H) The left graph shows that expression of this gene was reduced in *rdm4* mutant at all temperatures. The right graph shows strong induction of this gene in response to cold (10 °C and 2 °C) in wild type, and lesser induction by cold in *rdm4* mutant. (I, J) The left graphs show that expression of this gene is significantly increased in *rdm4* mutant at all temperatures. The right graphs show strong induction of this gene in response to cold in *rdm4* mutant.

factor 1- $\alpha$ , which showed a correlation with lysine increase (Habben et al., 1995), was significantly increased in rdm4 with lysine content of 10.5% (Supplementary Table S3). The analysis confirmed the substantial albeit distinct qualitative and quantitative increase in key lysine-rich non-zein proteins may contribute to lysine improvement in rdm4, although this lysine increase is less significant than that in o2 (Morton et al., 2016).

# Potential role of RDM4 in regulation of known cold-stress-responsive genes

RDM4 has been reported to be involved in the cold response in Arabidopsis, and affects the expression of several cold-stressresponsive genes, especially CBFs/DREBs via promoter occupancy (He et al., 2009). The RdDM pathway is not thought to be required for cold stress responses, and the association of RDM4 and Pol II is activated under chilling conditions (Chan et al., 2016). We observed more than 2000 cold-stressresponsive genes with significantly differential transcript expression in response to cold in WT, which were not significantly differentially regulated in rdm4, possibly suggesting an overarching function for RDM4 in abiotic stress tolerance (Figs 5D, 7, Supplementary Fig. S5). For example, inducer of ICE1 (Fig. 7E) is a master regulator of CBFs in cold stress, and mitogen-activated protein kinase 3 (MPK3, Supplementary Fig. S5D) negatively regulates CBF expression in plants (Li et al., 2017). ICE1, a bHLH transcription factor, was identified as an inducer of CBF expression and a key regulator of CBF genes under cold conditions (Li et al., 2016). Higher levels of superoxide dismutase (Fig. 7C) were found after freezing treatment in the overexpression of ICE1 (Zuo et al., 2019). Overexpression of the ABC transporter gene (Fig. 7D) increases abiotic stress tolerance in Arabidopsis (Chen et al., 2018). Glycerol-3-phosphate acyltransferase (Supplementary Fig. S5F) plays a pivotal role in cold resistance in a variety of plant species (Li et al., 2018b).

Jasmonic acid (JA) and its methylated ester, methyl jasmonate (MeJA), have been shown to control aspects of flowering, plant growth and development, and responses to various abiotic stresses (Huang et al., 2017). A lower DNA methylation level and significant up-regulation of the genes involved in JA biosynthesis were found in salt-tolerant line ND98 in sweet potato (Zhang et al., 2017). The JA pathway was involved in plant development and stunted plant growth was accompanied by increased jasmonate as a growth inhibitor (Zhang and Turner, 2008). In the CBF signaling pathway, epigenetic regulation plays an important role in modulating mRNA expression under cold stress (Ding et al., 2019), and RDM4 is important for Pol II occupancy at the promoters of CBF2 and CBF3 genes (Chan et al., 2016). Overexpression of JASMONATE ZIM-DOMAIN 1 (JAZ1, Supplementary Fig. S5I) or JAZ4 repressed freezing stress responses, and jasmonate acted as an upstream signal of the ICE-CBF transcriptional pathway to positively regulate freezing stress responses in Arabidopsis (Hu et al., 2013). JA was involved in leaf senescence and tolerance to cold stress (Hu et al., 2017). In this study, jasmonate O-methyltransferase and other jasmonate-induced genes were found significantly down-regulated in rdm4 mutant leaves

(see Supplementary Tables S4, S5). Based on the strong positive correlation and expression pattern, it is hypothesized that jasmonate-related mRNA expression is highly dependent on RDM4, and regulates the downstream cold stress responses and vegetative growth in maize leaves.

Histones had increased abundance in both proteomic and transcriptomic analysis in endosperm and seedling of rdm4 (Supplementary Table S3; Table 4; Fig. 7G) as had the histonerelated proteins such as histone deacetylase 2b (B6SK06). We observed a similar increase for NRPB1 in rdm4 mutant (Fig. 7F). RDM4 ortholog Iwr1 was found in yeast, and is important for the import of Pol II from the cytoplasm into the nucleus and its regulation (He et al., 2009). Interestingly, there is an expression increase for NRPB1, but a decrease for histone, in WT in response to cold stress (Fig. 7F, G). RDM4 interacts with Pol II, Pol IV, and Pol V in plants (He et al., 2009; Movahedi et al., 2015; Xie and Yu, 2015). RDM4 was shown with affinity with the largest Pol-IV subunit (NUCLEAR RNA POLYMERASE D1, NRPD1), RNA-DEPENDENT RNA POLYMERASE 2 (RDR2), CLASSY 1 (CLSY1), and SAWADEE HOMEODOMAIN HOMOLOG 1 (SHH1) (Law et al., 2011), which did not have significantly changed mRNA expression in rdm4 in this study.

In addition, the deletion in rdm4 mutant covers two genes, including AMP-binding-like protein (Zm00001d023238), which is also annotated as long chain acyl-CoA synthetase 6 (LACS6). LACS is a gene family with redundant roles involved in fatty acid metabolism, and multiple family members have been found, such as six in rodent and human (Teodoro et al., 2017), 34 in Brassica napus (Xiao et al., 2019), nine in Arabidopsis (Zhao et al., 2019), and nine in maize based on the annotation v4. The additional alleles and complementation tests showed that RDM4 is responsible for the seed, vegetative growth and male sterility phenotypes, although the loss of AMP-bindinglike protein might also contribute to differentially abundant mRNAs and proteins identified in RNA-seq and LC-MS/MS experiments, respectively. Further studies are needed to address the possible effects of the loss of Zm00001d023238.

The identification and molecular characterization of rdm4 has highlighted a potential overarching role for RDM4 in normal seed, vegetative and reproductive development as well as in stress responses in maize. Zein and non-zein proteins in kernels were significantly influenced by a loss of RDM4, which resulted in proteomic rebalancing analogous to but substantially different from that observed in o2. Global transcriptional changes were shown in endosperm and leaf, including many transcription factors. A radically altered transcriptome in the rdm4 mutant in response to cold may suggest an overarching function for RDM4 in abiotic stress tolerance. Studies to characterize possible roles for RDM4 in regulating the seed proteome and the transcriptional response to cold in terms of protein and nucleic acid interaction with RDM4, and whether or not DNA methylation is involved, are needed.

# Supplementary data

Supplementary data are available at *JXB* online.

- Fig. S1. Kernel segregation in *UniformMu* insertion lines for *RDM4* and AMP-binding like protein.
- Fig. S2. RT-PCR and qRT-PCR of candidate genes in developing endosperm.
- Fig. S3. Functional enrichment of DEGs in endosperm, seedling28, seedling10 and seedling2 by MapMan.
- Fig. S4. Phenotype of wild type and *rdm4* mutant seedlings by cold stress.
- Fig. S5. qRT-PCR for more candidate genes regulated by *RDM4* in response to cold stress in seedlings.
  - Table S1. Primers used in this study.
- Table S2. UFMU lines for RDM4 and AMP-binding like protein.
- Table S3. Proteins abundances and comparison in the proteomic analysis.
- Table S4. Differentially expressed genes in RNA-seq datasets. Table S5. Genes significantly correlated with RDM4 in all the seedling samples.

# **Acknowledgements**

The authors thank Drs Kan Liu, Peisheng Mao, and Weilong Yang for assistance with analysing data, and Drs Shahryar Kianian, Aixia Li, Kyla Morton and Lingling Yuan for helping with early work associated with the B73 mutant population. This work was supported by the Agriculture and Food Research Initiative competitive grant no. 2013–02278 of the USDA National Institute of Food and Agriculture to DH, the Chinese Universities Scientific Fund (2019TC257) to SJ, the Nebraska Research Initiative to SA and MN, the UNL Center for Plant Science Innovation Program of Excellence and the UNL Department of Agronomy and Horticulture to DH.

# **Author contributions**

SJ carried out field and lab work, conducted the data analysis and wrote the manuscript. AY and RA conducted amino acid profiling. MN and SA conducted the proteomics analysis. CZ participated in the design of the study and data analysis, and helped to write the manuscript. DH conceived and coordinated the study, carried out field and lab work, and wrote the manuscript. All authors read and approved the final manuscript.

## References

- Chan Z, Wang Y, Cao M, Gong Y, Mu Z, Wang H, Hu Y, Deng X, He XJ, Zhu JK. 2016. *RDM4* modulates cold stress resistance in *Arabidopsis* partially through the CBF-mediated pathway. New Phytologist **209**, 1527–1539.
- Chen N, Song B, Tang S, He J, Zhou Y, Feng J, Shi S, Xu X. 2018. Overexpression of the ABC transporter gene *TsABCG11* increases cuticle lipids and abiotic stress tolerance in *Arabidopsis*. Plant Biotechnology Reports 12, 303–313.
- **da Silva LS, Taylor J, Taylor JR.** 2011. Transgenic sorghum with altered kafirin synthesis: kafirin solubility, polymerization, and protein digestion. Journal of Agricultural and Food Chemistry **59**, 9265–9270.
- **Ding Y, Shi Y, Yang S.** 2019. Advances and challenges in uncovering cold tolerance regulatory mechanisms in plants. New Phytologist **222**, 1690–1704.
- **Guo X, Yuan L, Chen H, Sato SJ, Clemente TE, Holding DR.** 2013. Nonredundant function of zeins and their correct stoichiometric ratio drive protein body formation in maize endosperm. Plant Physiology **162**, 1359–1369.

- **Habben JE, Moro GL, Hunter BG, Hamaker BR, Larkins BA.** 1995. Elongation factor 1 alpha concentration is highly correlated with the lysine content of maize endosperm. Proceedings of the National Academy of Sciences, USA **92**, 8640–8644.
- He XJ, Hsu YF, Zhu S, Liu HL, Pontes O, Zhu J, Cui X, Wang CS, Zhu JK. 2009. A conserved transcriptional regulator is required for RNA-directed DNA methylation and plant development. Genes & Development 23. 2717–2722.
- **Holding DR.** 2014. Recent advances in the study of prolamin storage protein organization and function. Frontiers in Plant Science **5**, 276.
- **Holding DR, Larkins BA.** 2006. The development and importance of zein protein bodies in maize endosperm. Maydica **51**, 243.
- **Holding DR, Messing J.** 2013. Evolution, structure, and function of prolamin storage proteins. In: Becraft PW, ed. Seed genomics. New York: John Wiley & Sons, 138–158.
- Holding DR, Otegui MS, Li B, Meeley RB, Dam T, Hunter BG, Jung R, Larkins BA. 2007. The maize floury1 gene encodes a novel endoplasmic reticulum protein involved in zein protein body formation. The Plant Cell 19, 2569–2582.
- **Hu Y, Jiang L, Wang F, Yu D.** 2013. Jasmonate regulates the INDUCER OF CBF EXPRESSION-C-REPEAT BINDING FACTOR/DRE BINDING FACTOR1 cascade and freezing tolerance in *Arabidopsis*. The Plant Cell **25**, 2907–2924.
- **Hu Y, Jiang Y, Han X, Wang H, Pan J, Yu D.** 2017. Jasmonate regulates leaf senescence and tolerance to cold stress: crosstalk with other phytohormones. Journal of Experimental Botany **68**, 1361–1369.
- **Huang H, Liu B, Liu L, Song S.** 2017. Jasmonate action in plant growth and development. Journal of Experimental Botany **68**, 1349–1359.
- **Jia M, Wu H, Clay KL, Jung R, Larkins BA, Gibbon BC.** 2013. Identification and characterization of lysine-rich proteins and starch biosynthesis genes in the *opaque2* mutant by transcriptional and proteomic analysis. BMC Plant Biology **13**, 60.
- Jia S, Li A, Morton K, Avoles-Kianian P, Kianian SF, Zhang C, Holding D. 2016. A population of deletion mutants and an integrated mapping and exome-seq pipeline for gene discovery in maize. G3 6, 2385–2395.
- **Jia S, Li A, Zhang C, Holding D.** 2018a. Deletion mutagenesis and identification of causative mutations in maize. Methods in Molecular Biology **1676**, 97–108.
- **Jia S, Morton K, Zhang C, Holding D.** 2018*b*. An exome-seq based tool for mapping and selection of candidate genes in maize deletion mutants. Genomics, Proteomics & Bioinformatics **16**, 439–450.
- **Kanno T, Bucher E, Daxinger L, et al.** 2010. RNA-directed DNA methylation and plant development require an IWR1-type transcription factor. EMBO Reports **11**, 65–71.
- **Kawakatsu T, Hirose S, Yasuda H, Takaiwa F.** 2010. Reducing rice seed storage protein accumulation leads to changes in nutrient quality and storage organelle formation. Plant Physiology **154**, 1842–1854.
- Kim CS, Woo Ym YM, Clore AM, Burnett RJ, Carneiro NP, Larkins BA. 2002. Zein protein interactions, rather than the asymmetric distribution of zein mRNAs on endoplasmic reticulum membranes, influence protein body formation in maize endosperm. The Plant Cell 14, 655–672.
- Kim D, Pertea G, Trapnell C, Pimentel H, Kelley R, Salzberg SL. 2013. TopHat2: accurate alignment of transcriptomes in the presence of insertions, deletions and gene fusions. Genome Biology 14, R36.
- **Law JA, Vashisht AA, Wohlschlegel JA, Jacobsen SE.** 2011. SHH1, a homeodomain protein required for DNA methylation, as well as RDR2, RDM4, and chromatin remodeling factors, associate with RNA polymerase IV. PLoS Genetics **7**, e1002195.
- **Layer RM, Chiang C, Quinlan AR, Hall IM.** 2014. LUMPY: a probabilistic framework for structural variant discovery. Genome Biology **15**, R84.
- **Lending CR, Larkins BA.** 1989. Changes in the zein composition of protein bodies during maize endosperm development. The Plant Cell **1**, 1011-1023.
- **Li A, Jia S, Yobi A, Ge Z, Sato SJ, Zhang C, Angelovici R, Clemente TE, Holding DR.** 2018a. Editing of an Alpha-Kafirin gene family increases, digestibility and protein quality in sorghum. Plant Physiology **177**, 1425–1438.
- **Li C, Song R.** 2020. The regulation of zein biosynthesis in maize endosperm. Theoretical and Applied Genetics **133**, 1443–1453.

- Li C, Qiao Z, Qi W, et al. 2015. Genome-wide characterization of cisacting DNA targets reveals the transcriptional regulatory framework of opaque2 in maize. The Plant Cell 27, 532-545.
- Li H, Ding Y, Shi Y, Zhang X, Zhang S, Gong Z, Yang S. 2017. MPK3and MPK6-mediated ICE1 phosphorylation negatively regulates ICE1 stability and freezing tolerance in Arabidopsis. Developmental Cell 43, 630-642.e4.
- Li X. Liu P. Yang P. Fan C. Sun X. 2018b. Characterization of the alveerol-3-phosphate acyltransferase gene and its real-time expression under cold stress in Paeonia lactiflora Pall. PLoS One 13, e0202168.
- Li Z, Hu G, Liu X, et al. 2016. Transcriptome sequencing identified genes and gene ontologies associated with early freezing tolerance in maize. Frontiers in Plant Science 7, 1477.
- Love MI, Huber W, Anders S. 2014. Moderated estimation of fold change and dispersion for RNA-seq data with DESeq2. Genome Biology 15, 550.
- Matzke MA, Kanno T, Matzke AJ. 2015. RNA-directed DNA methylation: the evolution of a complex epigenetic pathway in flowering plants. Annual Review of Plant Biology 66, 243-267.
- Mertz ET, Bates LS, Nelson OE. 1964. Mutant gene that changes protein composition and increases lysine content of maize endosperm. Science
- Moro GL, Habben JE, Hamaker BR, Larkins BA. 1996. Characterization of the variability in lysine content for normal and opaque2 maize endosperm. Crop Science 36, 1651-1659.
- Morton KJ, Jia S, Zhang C, Holding DR. 2016. Proteomic profiling of maize opaque endosperm mutants reveals selective accumulation of lysineenriched proteins. Journal of Experimental Botany 67, 1381-1396.
- Movahedi A, Sun W, Zhang J, Wu X, Mousavi M, Mohammadi K, Yin T, Zhuge Q. 2015. RNA-directed DNA methylation in plants. Plant Cell Reports 34, 1857-1862.
- Schmidt MA, Herman EM. 2008. Proteome rebalancing in soybean seeds can be exploited to enhance foreign protein accumulation. Plant Biotechnology Journal 6, 832-842.
- Schmidt RJ, Burr FA, Aukerman MJ, Burr B. 1990. Maize regulatory gene opaque-2 encodes a protein with a "leucine-zipper" motif that binds to zein DNA. Proceedings of the National Academy of Sciences, USA 87, 46-50.
- Takaiwa F, Yang L, Wakasa Y, Ozawa K. 2018. Compensatory rebalancing of rice prolamins by production of recombinant prolamin/bioactive peptide fusion proteins within ER-derived protein bodies. Plant Cell Reports 37, 209–223.
- Teodoro BG, Sampaio IH, Bomfim LH, Queiroz AL, Silveira LR, Souza AO, Fernandes AM, Eberlin MN, Huang TY, Zheng D. 2017. Long-chain acyl-CoA synthetase 6 regulates lipid synthesis and mitochondrial oxidative capacity in human and rat skeletal muscle. Journal of Physiology **595**, 677–693.
- Trapnell C. Roberts A. Goff L. Pertea G. Kim D. Kellev DR. Pimentel H. Salzberg SL, Rinn JL, Pachter L. 2012. Differential gene and transcript expression analysis of RNA-seq experiments with TopHat and Cufflinks. Nature Protocols 7, 562-578.
- Usadel B, Nagel A, Steinhauser D, et al. 2006. PageMan: an interactive ontology tool to generate, display, and annotate overview graphs for profiling experiments. BMC Bioinformatics 7, 535.

- Usadel B, Poree F, Nagel A, Lohse M, Czedik-Eysenberg A, Stitt M. 2009. A guide to using MapMan to visualize and compare Omics data in plants: a case study in the crop species, Maize. Plant, Cell & Environment **32**, 1211-1229.
- Wallace JC, Lopes MA, Paiva E, Larkins BA. 1990. New methods for extraction and quantitation of zeins reveal a high content of y-zein in modified opaque-2 maize. Plant Physiology 92, 191-196.
- Wang G. Wang F. Wang G. et al. 2012. Opaque1 encodes a myosin XI motor protein that is required for endoplasmic reticulum motility and protein body formation in maize endosperm. The Plant Cell 24, 3447-3462.
- Woo YM, Hu DW, Larkins BA, Jung R. 2001. Genomics analysis of genes expressed in maize endosperm identifies novel seed proteins and clarifies patterns of zein gene expression. The Plant Cell 13, 2297-2317.
- Wu Y, Messing J. 2010. RNA interference-mediated change in protein body morphology and seed opacity through loss of different zein proteins. Plant Physiology **153**, 337–347.
- Wu Y. Messing J. 2014. Proteome balancing of the maize seed for higher nutritional value. Frontiers in Plant Science 5, 240.
- Xiao Z, Li N, Wang S, et al. 2019. Genome-wide identification and comparative expression profile analysis of the long-chain Acyl-CoA synthetase (LACS) gene family in two different oil content cultivars of Brassica napus. Biochemical Genetics 57, 781–800.
- Xie M. Yu B. 2015. siRNA-directed DNA methylation in plants. Current Genomics 16, 23-31.
- Yang F, Shen Y, Camp DG 2nd, Smith RD. 2012. High-pH reversedphase chromatography with fraction concatenation for 2D proteomic analysis. Expert Review of Proteomics 9, 129-134.
- Yobi A, Angelovici R. 2018. A high-throughput absolute-level quantification of protein-bound amino acids in seeds. Current Protocols in Plant Biology 3, e20084.
- Zhang H, Zhang Q, Zhai H, Li Y, Wang X, Liu Q, He S. 2017. Transcript profile analysis reveals important roles of jasmonic acid signalling pathway in the response of sweet potato to salt stress. Scientific Reports **7**, 40819.
- Zhang Y, Turner JG. 2008. Wound-induced endogenous jasmonates stunt plant growth by inhibiting mitosis. PLoS One 3, e3699.
- Zhang Z, Yang J, Wu Y. 2015. Transcriptional regulation of zein gene expression in maize through the additive and synergistic action of opaque2, prolamine-box binding factor, and O2 heterodimerizing proteins. The Plant cell 27, 1162-1172.
- Zhang Z, Zheng X, Yang J, Messing J, Wu Y. 2016. Maize endospermspecific transcription factors O2 and PBF network the regulation of protein and starch synthesis. Proceedings of the National Academy of Sciences, USA 113, 10842-10847.
- Zhao L, Haslam TM, Sonntag A, Molina I, Kunst L. 2019. Functional overlap of long-chain Acyl-CoA synthetases in Arabidopsis. Plant & Cell Physiology 60, 1041-1054.
- Zuo Z, Kang H, Park M, Jeong H, Sun H, Yang D, Lee Y, Song P, Lee H. 2019. Overexpression of ICE1, a regulator of cold-induced transcriptome, confers cold tolerance to transgenic Zoysia japonica. Journal of Plant Biology 62, 137-146.